



# Syntheses, structural diversities and magnetic properties of four new Co(II) coordination polymers with phthalic acid derivatives

Shi-Yuan Zhang, Na Xu<sup>\*</sup>, Wei Shi, Peng Cheng, Dai-Zheng Liao

Department of Chemistry, Key Laboratory of Advanced Energy Material Chemistry, MOE, and TKL of Metal and Molecule Based Material Chemistry, Nankai University, Tianjin 300071, PR China

## ARTICLE INFO

### Article history:

Received 1 August 2012

Accepted 21 December 2012

Available online 11 January 2013

### Keywords:

Co(II) coordination polymer

Phthalic acid

Crystal structure

Magnetic property

## ABSTRACT

Four new 3D Co(II) coordination polymers, [Co(4apa)(H<sub>2</sub>O)] (**1**), [Co(bpy)(3npa)] (**2**), [Co(bpy)<sub>1.5</sub>(3adpa)] (**3**) and [Co(btx)<sub>0.5</sub>(4npa)(H<sub>2</sub>O)<sub>2</sub>] (**4**) (H<sub>2</sub>4apa = 4-aminophthalic acid, bpy = 4,4'-bipyridine, H<sub>2</sub>3npa = 3-nitrophthalic acid, H<sub>2</sub>3adpa = 3-(4-amino-1,3-dioxoisindolin-2-yl)phthalic acid, btx = 1,4-bis(1,2,4-triazole-1-ylmethyl)benzene, H<sub>2</sub>4npa = 4-nitrophthalic acid), have been synthesized and characterized by single crystal X-ray diffraction, PXRD and magnetic susceptibility measurements. An interesting *in situ* acylation reaction of 3-aminophthalic acid (H<sub>2</sub>3apa) has been found in the formation of coordination polymer **3**. The Co(II) ions of each polymer lie in distorted octahedral environments and are bridged by  $\mu_{1,3}$  carboxylate groups to form 2D (**1**), 1D (**2** and **3**) and dimer (**4**) structures, which are further assembled through ligands into different 3D structures due to the influence of the substituent groups. Studies of the temperature dependence of the magnetic susceptibilities in the range 2–300 K reveal antiferromagnetic interactions in **1–4** between the Co(II) ions transmitted by  $\mu_{1,3}$  carboxylate groups.

© 2013 Elsevier Ltd. All rights reserved.

## 1. Introduction

Functional coordination polymers have attracted considerable attention in the past decades due to their valuable properties, such as magnetism [1], luminescence [2], catalysis [3], and adsorption [4]. In this context, magnetic coordination polymers are of special interest. The magnetic properties of coordination polymers are attributed to (i) spin carriers such as metal ions providing the source of magnetic moments, and (ii) different bridging ligands providing superexchange pathways between the spin carriers. To better understand the magnetic properties of coordination polymers there have been many efforts in the strategy of synthesis and analysis of magneto-structural correlations [1,5], but it is still a great challenge to assemble spin carriers to the skeleton of coordination polymers with predetermined structures and targeted magnetic properties. The way to solve of this problem lies in the understanding of magneto-structural correlations more thoroughly through both experimental and theoretical investigations.

Co(II) ion is one of the interesting candidates of spin carriers and usually leads to fascinating magnetic properties. In an octahedral coordination geometry, its magnetic moment includes contributions from not only the spin angular momentum but also the orbital angular momentum, different from other first-row transition metal ions whose orbital angular momentums are always

quenched by the ligand field. On the other hand, carboxylate ligands exhibit an extensively documented ability to bridge metal ions, forming 1D, 2D and 3D coordination networks [1a,f,6]. Carboxylate groups can adopt many types of bridging conformations, such as triatomic *syn-syn*, *anti-syn*, and *anti-anti*. Ferro- or antiferromagnetic interactions can be effectively transmitted through such three atom bridges [7]. However, due to the structural diversities of Co(II) coordination polymers, a detailed understanding of magneto-structural correlations in such systems is still unclear [1c]. Our previous studies show that phthalic acid is a good bridging ligand to build molecular magnetic materials due to its flexibility of coordination modes [8]. As a continuation of this work, four phthalic acid derivatives (H<sub>2</sub>4apa = 4-aminophthalic acid, H<sub>2</sub>3npa = 3-nitrophthalic acid, H<sub>2</sub>3apa = 3-aminophthalic acid, H<sub>2</sub>4npa = 4-nitrophthalic acid) were selected because of their abilities to adopt various coordination modes like phthalic acid but with different substituent groups. It is noted that H<sub>2</sub>3adpa (H<sub>2</sub>3adpa = 3-(4-amino-1,3-dioxoisindolin-2-yl)phthalic acid) was formed by the *in situ* acylation reaction of 3-aminophthalic acid (H<sub>2</sub>3apa) in the formation of coordination polymer **3**. Furthermore, net neutral linear linkers 4,4'-bipyridine (bpy) and 1,4-bis(1,2,4-triazole-1-ylmethyl)benzene (btx) were employed as co-ligands. Four new 3D coordination polymers, [Co(4apa)(H<sub>2</sub>O)] (**1**), [Co(bpy)(3npa)] (**2**), [Co(bpy)<sub>1.5</sub>(3adpa)] (**3**) and [Co(btx)<sub>0.5</sub>(4npa)(H<sub>2</sub>O)<sub>2</sub>] (**4**), were successfully synthesized and characterized. Studies of the temperature dependence of the magnetic susceptibilities in the range 2–300 K reveal antiferromagnetic interactions in **1–4**

<sup>\*</sup> Corresponding author.

E-mail address: [naxu@nankai.edu.cn](mailto:naxu@nankai.edu.cn) (N. Xu).

between the Co(II) ions transmitted by the *anti-syn* carboxylate groups.

## 2. Experimental

### 2.1. General considerations

All reagents and solvents employed were commercially available and used as received without further purification. Elemental analyses for C, H and N were performed on a Perkin-Elmer 240 CHN elemental analyzer. Powder X-ray diffraction measurements were measured on a D/Max-2500 X-ray diffractometer using Cu K $\alpha$  radiation. Variable-temperature magnetic susceptibilities were measured on a SQUID MPMS XL-7 magnetometer. Diamagnetic corrections were made with Pascal's constants for all the constituent atoms and sample holders.

### 2.2. Syntheses

#### 2.2.1. [Co(4apa)(H<sub>2</sub>O)] (1)

A mixture of Co(NO<sub>3</sub>)<sub>2</sub>·6H<sub>2</sub>O (0.116 g, 0.40 mmol), 4-aminophthalic acid (0.054 g, 0.30 mmol), NaOH (0.016 g, 0.40 mmol) and H<sub>2</sub>O (10 mL) was sealed in a 25 mL Teflon-lined stainless steel vessel and heated at 150 °C for 2 days, and then cooled to room temperature. Red block-shaped crystals were filtered off, washed with water and dried in air. Yield: 67% based on 4apa. *Anal.* Calc. for C<sub>8</sub>H<sub>9</sub>CoNO<sub>5</sub> (258.08): C, 37.23; H, 3.51; N, 5.43. Found: C, 37.45; H, 3.80; N, 5.59%.

#### 2.2.2. [Co(bpy)(3npa)] (2)

A mixture of Co(NO<sub>3</sub>)<sub>2</sub>·6H<sub>2</sub>O (0.116 g, 0.40 mmol), 4,4'-bipyridine (0.016 g, 0.10 mmol), 3-nitrophthalic acid (0.042 g, 0.20 mmol), NaOH (0.008 g, 0.20 mmol) and H<sub>2</sub>O (10 mL) was sealed in a 25 mL Teflon-lined stainless steel vessel and heated at 150 °C for 2 days, and then cooled to room temperature. Red block-shaped crystals were filtered off, washed with water and

dried in air. Yield: 76% based on bpy. *Anal.* Calc. for C<sub>18</sub>H<sub>11</sub>CoN<sub>3</sub>O<sub>6</sub> (424.23): C, 50.96; H, 2.61; N, 9.91. Found: C, 50.96; H, 2.62; N, 9.79%.

#### 2.2.3. [Co(bpy)<sub>1.5</sub>(3adpa)] (3)

A mixture of Co(NO<sub>3</sub>)<sub>2</sub>·6H<sub>2</sub>O (0.116 g, 0.40 mmol), 4,4'-bipyridine (0.048 g, 0.30 mmol), 3-aminophthalic acid (0.054 g, 0.30 mmol), NaOH (0.016 g, 0.40 mmol) and H<sub>2</sub>O (10 mL) was sealed in a 25 mL Teflon-lined stainless steel vessel and heated at 150 °C for 2 days, and then cooled to room temperature. Red block-shaped crystals were filtered off, washed with water and dried in air. Yield: 64% based on bpy. *Anal.* Calc. for C<sub>31</sub>H<sub>20</sub>CoN<sub>5</sub>O<sub>6</sub> (617.45): C, 60.30; H, 3.26; N, 11.34. Found: C, 60.04; H, 3.74; N, 11.56%.

#### 2.2.4. [Co(btx)<sub>0.5</sub>(4npa)(H<sub>2</sub>O)<sub>2</sub>] (4)

A mixture of Co(NO<sub>3</sub>)<sub>2</sub>·6H<sub>2</sub>O (0.116 g, 0.40 mmol), 1,4-bis(1,2,4-triazol-1-ylmethyl) benzene (0.024 g, 0.10 mmol), 4-nitrophthalic acid (0.042 g, 0.20 mmol), NaOH (0.008 g, 0.20 mmol) and H<sub>2</sub>O (10 mL) was sealed in a 25 mL Teflon-lined stainless steel vessel and heated at 150 °C for 2 days, and then cooled to room temperature. Red block-shaped crystals were filtered off, washed with water and dried in air. Yield: 73% based on btx. *Anal.* Calc. for C<sub>14</sub>H<sub>13</sub>CoN<sub>4</sub>O<sub>8</sub> (424.21): C, 39.64; H, 3.09; N, 13.21. Found: C, 39.78; H, 3.00; N, 12.98%.

### 2.3. Crystal structure determination

Diffraction data of the four compounds were collected at 150 or 293 K on an Oxford Supernova diffractometer equipped with graphite-monochromated Mo K $\alpha$  radiation ( $\lambda = 0.71073$  Å) using the  $\omega$ -scan technique. Lorentz polarization and absorption corrections were applied. The structures were solved by the direct method and refined with the full-matrix least-squares technique using the SHELXTL program package [9]. Anisotropic thermal parameters were assigned to all non-hydrogen atoms. The hydrogen atoms were set in calculated positions and refined as riding atoms with

**Table 1**  
Data collection and processing parameters for 1–4.

	1	2	3	4
Formula	C <sub>8</sub> H <sub>9</sub> CoNO <sub>5</sub>	C <sub>18</sub> H <sub>11</sub> CoN <sub>3</sub> O <sub>6</sub>	C <sub>31</sub> H <sub>20</sub> CoN <sub>5</sub> O <sub>6</sub>	C <sub>14</sub> H <sub>13</sub> CoN <sub>4</sub> O <sub>8</sub>
Formula weight	256.08	424.23	617.45	424.21
T (K)	150(2)	150(2)	293(2)	150(2)
Crystal system	monoclinic	monoclinic	monoclinic	monoclinic
Space group	P2(1)/c	P2(1)/n	P21/c	C2/c
a (Å)	10.3115(4)	7.1044(8)	11.5656(5)	37.186(3)
b (Å)	7.3868(3)	23.403(2)	21.4632(6)	5.9373(4)
c (Å)	14.2596(7)	10.8747(15)	11.8959(5)	14.9209(9)
$\alpha$ (°)	90	90	90	90
$\beta$ (°)	126.966(3)	113.173(10)	108.644(4)	112.981(8)
$\gamma$ (°)	90	90	90	90
V (Å <sup>3</sup> )	867.82(6)	1662.2(3)	2798.01(19)	3032.8(4)
Z	4	4	1	8
$\rho$ (g/cm <sup>3</sup> )	1.960	1.695	1.466	1.858
$\mu$ (mm <sup>-1</sup> )	1.977	1.078	0.668	1.192
$\theta$ (°)	2.88–25.99	2.68–26.00	2.62–25.01	2.38–25.50
Index ranges	–12 ≤ h ≤ 12, –9 ≤ k ≤ 8, –17 ≤ l ≤ 17	–8 ≤ h ≤ 4, –28 ≤ k ≤ 21, –12 ≤ l ≤ 13	–13 ≤ h ≤ 13, –25 ≤ k ≤ 24, –9 ≤ l ≤ 14	–44 ≤ h ≤ 44, –7 ≤ k ≤ 5, –17 ≤ l ≤ 18
Reflections collected	3334	6888	10418	5769
Independent reflections	1707 (0.0282)	3269 (0.0282)	4930 (0.0282)	2810 (0.0282)
$R_{int}$				
Data/restraints/parameters	1707/0/140	3269/24/253	4930/15/389	2810/0/256
Goodness-of-fit (GOF) on $F^2$	1.044	0.949	1.062	1.016
$R_1$ , $\omega R_2$ [ $I > 2\sigma(I)$ ]	0.0356, 0.0846	0.0560, 0.1432	0.0801, 0.2429	0.0316, 0.0741
$R_1$ , $\omega R_2$ (all data)	0.0425, 0.0872	0.0987, 0.1832	0.1263, 0.2643	0.0410, 0.0770

**Table 2**  
Selected bond lengths (Å) for **1–4**.

<b>1<sup>a</sup></b>				<b>2<sup>b</sup></b>			
Co(1)–O(4)#1	2.035(2)	Co(1)–O(3)#2	2.093(2)	Co(1)–O(2)#1	2.051(4)	Co(1)–O(4)#2	2.098(4)
Co(1)–O(1)	2.073(2)	Co(1)–O(5)	2.136(2)	Co(1)–O(3)	2.074(4)	Co(1)–N(2)#3	2.142(4)
Co(1)–O(2)#2	2.091(2)	Co(1)–N(1)#3	2.210(3)	Co(1)–O(1)	2.086(3)	Co(1)–N(1)	2.187(4)
<b>3<sup>c</sup></b>				<b>4<sup>d</sup></b>			
Co(1)–O(3)	2.104(4)	Co(1)–N(1)#2	2.129(6)	Co(1)–O(1)#1	2.0740(15)	Co(1)–N(1)	2.1268(19)
Co(1)–O(2)#1	2.106(4)	Co(1)–O(1)	2.149(4)	Co(1)–O(4)#2	2.0777(15)	Co(1)–O(8)	2.1287(18)
Co(1)–N(2)	2.123(6)	Co(1)–N(3)	2.190(5)	Co(1)–O(3)	2.1042(14)	Co(1)–O(7)	2.1352(18)

<sup>a</sup> Symmetry transformations used to generate equivalent atoms: #1  $x, -y+1/2, z-1/2$ ; #2  $-x+2, y-1/2, -z+1/2$ ; #3  $-x+1, -y, -z$ .

<sup>b</sup> Symmetry transformations used to generate equivalent atoms: #1  $-x+1, -y, -z+1$ ; #2  $-x+2, -y, -z+1$ ; #3  $x+1, -y+1/2, z+1/2$ .

<sup>c</sup> Symmetry transformations used to generate equivalent atoms: #1  $x, -y+1/2, z-1/2$ ; #2  $x-1, -y+1/2, z-1/2$ .

<sup>d</sup> Symmetry transformations used to generate equivalent atoms: #1  $x, -y+1, z-1/2$ ; #2  $-x+1/2, -y+3/2, -z+1$ .

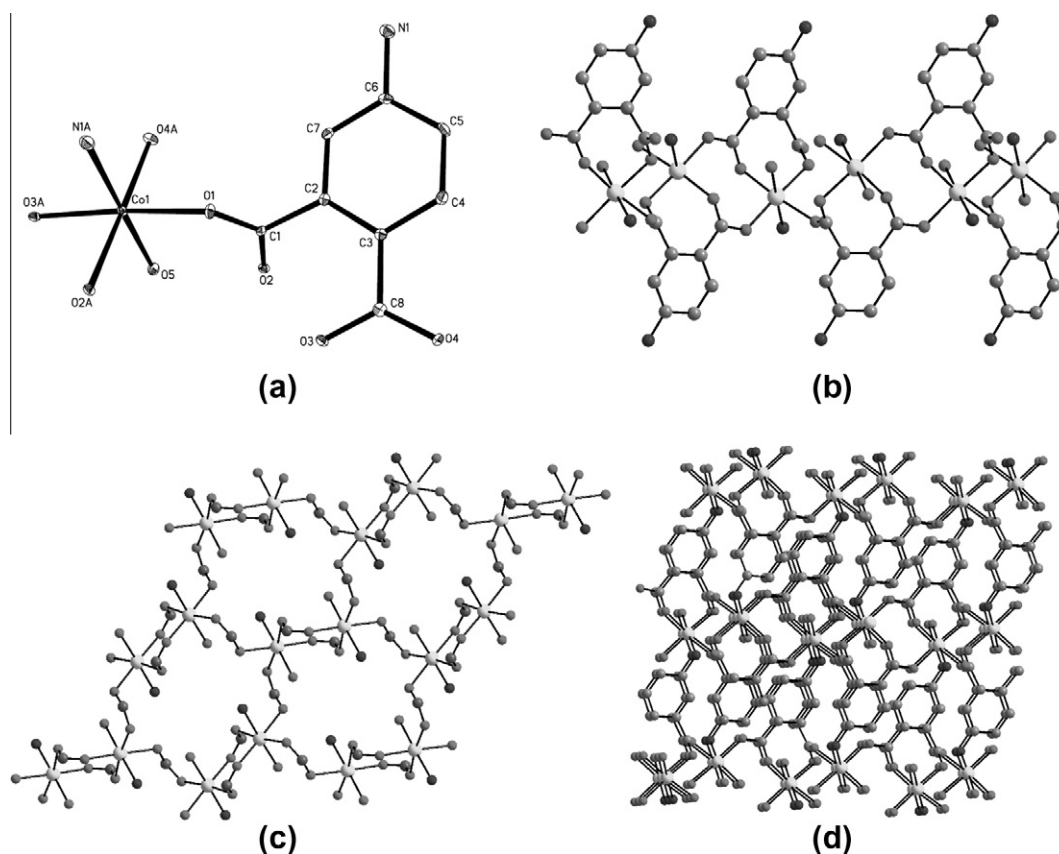


**Fig. 1.** (a) ORTEP plot of  $[\text{Co}(4\text{apa})(\text{H}_2\text{O})]$  (**1**). Thermal ellipsoids are shown at 30% probability. (b) The 1D structure in **1**. (c) The 2D structure formed by  $\mu_{1,3}$ -carboxylate bridges. (d) The 3D network of **1**. All H atoms are omitted for clarity.

a common fixed isotropic thermal parameter. The crystallographic data, bond lengths and selected angles of **1–4** are listed in Tables 1 and 2 and S1, respectively.

### 3. Results and discussion

#### 3.1. Structural description

##### 3.1.1. $[\text{Co}(4\text{apa})(\text{H}_2\text{O})]$ (**1**)

As shown in Fig. 1a, the Co(II) ion is six-coordinated and located in a slightly distorted octahedral environment surrounded by five O atoms (O1, O2A, O3A and O4A from the carboxylate groups of  $4\text{apa}^{2-}$  anions; O5 from the  $\text{H}_2\text{O}$  molecule) and one N atom (N1A from the amino group of the  $4\text{apa}^{2-}$  anion). The Co–O bond lengths are in the range 2.035–2.136 Å and the Co–N bond length is

2.210 Å. The  $\mu_{1,3}$ -carboxylate group links adjacent Co(II) ion in the *anti-syn* mode. The neighboring Co(II) ions are linked by double and single  $\mu_{1,3}$ -bridging carboxylate groups in an alternating way, forming a 1D structure with Co···Co distances of 4.3804 and 4.8425 Å, respectively (Fig. 1b). A 2D structure is formed in the *bc* plane via the connection of  $\mu_{1,3}$ -carboxylate bridges (Fig. 1c). The layers are further linked by the amino and carboxylate groups of  $4\text{apa}^{2-}$ , forming a 3D framework (Fig. 1d).

##### 3.1.2. $[\text{Co}(\text{bpy})(3\text{npa})]$ (**2**)

The central Co(II) ion is surrounded by four oxygen atoms (O1, O2A, O3 and O4A) from the carboxylate groups of  $3\text{npa}^{2-}$  and two nitrogen atoms (N1 and N2A) from bpy in a slightly distorted octahedral geometry (Fig. 2a). The nitro group of  $3\text{npa}^{2-}$  does not coordinate to the Co(II) ions. The Co–O and Co–N bond lengths are in the ranges 2.051–2.098 Å and 2.142–2.187 Å, respectively. Each

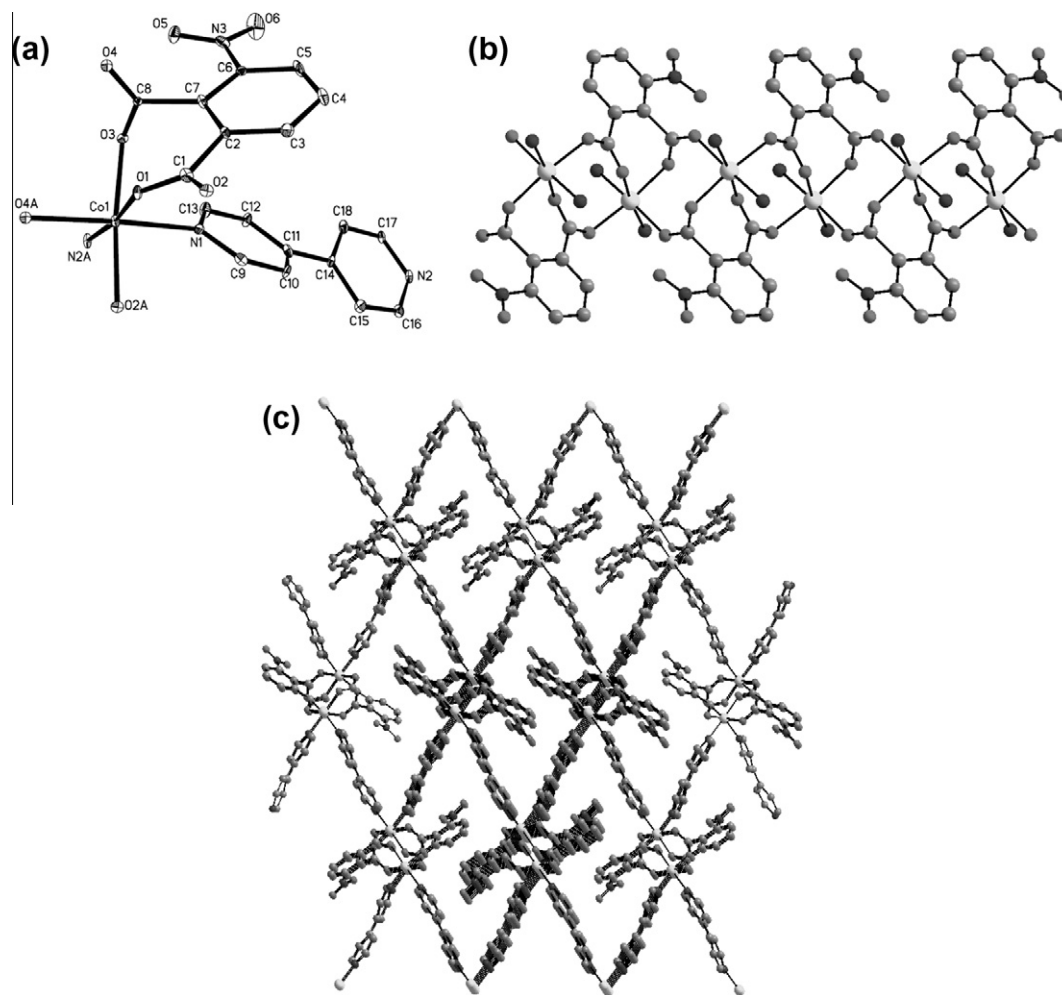
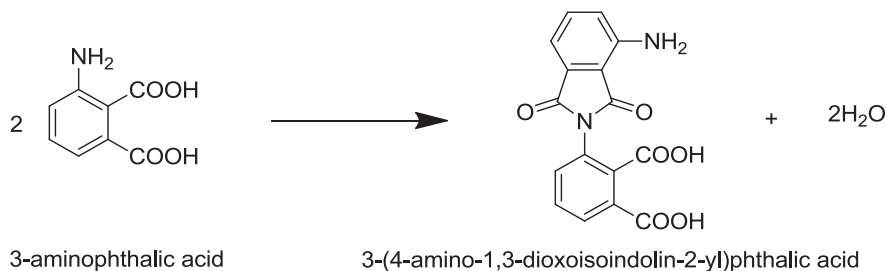


**Fig. 2.** (a) ORTEP plot of  $[\text{Co}(\text{bpy})(3\text{npa})]$  (**2**). Thermal ellipsoids are shown at 30% probability. (b) The 1D structure in **2**. All bpy ligands are omitted for clarity. (c) The 3D structure of **2**. All H atoms are omitted for clarity.



**Scheme 1.** *In situ* acylation reaction of 3-aminophthalic acid to give 3-(4-amino-1,3-dioxoisindolin-2-yl) phthalic acid.

$\mu_{1,3}$ -carboxylate group links adjacent Co(II) ions in *anti-syn* mode. Two adjacent Co(II) ions are connected by double  $\mu_{1,3}$ -carboxylate bridges to form a 1D structure along the *a* axis with Co···Co distances of 4.4996(3) and 4.8375(4) Å (Fig. 2b). The chains are further connected via bpy in the *bc* plane, resulting in a 3D coordination network (Fig. 2c).

### 3.1.3. $[\text{Co}(\text{bpy})_{1.5}(\text{3adpa})]$ (**3**)

Single crystal X-ray diffraction reveals that a hydrothermal *in situ* acylation reaction of 3-aminophthalic acid ( $\text{H}_2\text{3apa}$ ) to give 3-(4-amino-1,3-dioxoisindolin-2-yl)phthalic acid ( $\text{H}_2\text{3adpa}$ )

(Scheme 1) occurred during the formation of **3**. The Co(II) ion lies in a slightly distorted octahedral coordination geometry, surrounded by three O atoms (O1, O2A and O3) from the carboxylate groups of  $3\text{adpa}^{2-}$  and three N atoms (N1A, N2 and N3) from bpy (Fig. 3a). The Co–O and Co–N bond lengths are in the ranges 2.104–2.149 Å and 2.129–2.190 Å, respectively. Adjacent Co(II) ions are bridged by a  $\mu_{1,3}$ -carboxylate group in the *anti-syn* mode to form a 1D structure along the *c* axis (Fig. 3b) with adjacent Co···Co distances of 5.9587(2) and 5.9628(2) Å. The chains are further linked by bpy ligands, forming a 3D coordination network (Fig. 3c).

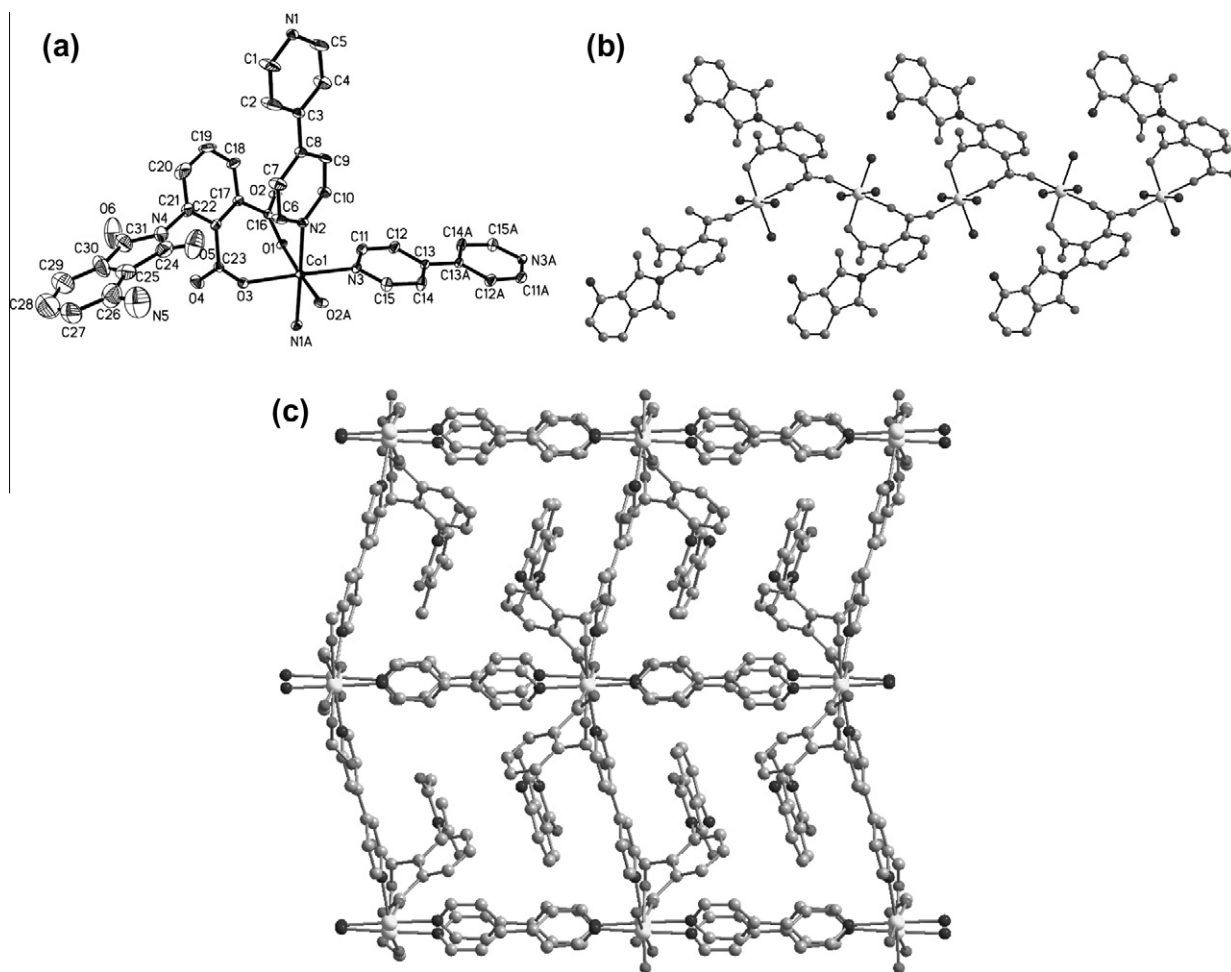


**Fig. 3.** (a) ORTEP plot of  $[\text{Co}(\text{bpy})_{1.5}(\text{3adpa})]$  (**3**). Thermal ellipsoids are shown at 30% probability. (b) The 1D Co–COO–Co structure in **3**. (c) The 3D structure of **3**. All H atoms are omitted for clarity.

### 3.1.4. $[\text{Co}(\text{btx})_{0.5}(\text{4npa})(\text{H}_2\text{O})_2]$ (**4**)

The Co(II) ion is coordinated by five O atoms (O1A, O3 and O4A from the carboxylate groups of  $4\text{npa}^{2-}$  anions; O7 and O8 from  $\text{H}_2\text{O}$  molecules) and one N atom (N1) from btx (Fig. 4a) to form a slightly distorted octahedral environment. Similar to **2**, the nitro group of  $4\text{npa}^{2-}$  does not coordinate to the Co(II) ions. The Co–O bond lengths are in the range 2.0740–2.1352 Å and Co–N bond length is 2.1268 Å. Two neighboring Co(II) ions are bridged by two  $\mu_{1,3}$ -carboxylate groups in the *anti-syn* mode to form a dimer structure with a Co···Co distance of 4.7592(5) Å. The dimers are connected by the carboxylate groups from two  $4\text{npa}^{2-}$  anions, forming a chain along the *c* axis with a nearest Co···Co distance (between dimers) of 5.6817(3) Å (Fig. 4b). In the *bc* plane, the dimers (polyhedrons in Fig. 4c) are linked via  $\mu_{1,3}$ -carboxylate groups of  $4\text{npa}^{2-}$  to form 2D structures, which are further linked by btx, forming a 3D framework (Fig. 4d).

The substituent group of phthalic acid plays an important role in the final structure. As shown in Scheme 2A and B, the two carboxylate groups of 4-aminophthalic acid or 3-nitrophthalic acid bridge three Co(II) ions in a  $\mu_2\text{-}\eta^1\text{:}\eta^1$  fashion. The difference in the coordination mode of the two ligands is the additional coordination bond between the amino group and the Co(II) ions in **1**. Due to the position of the amino group, neighboring Co(II) ions are linked by double and single  $\mu_{1,3}$ -bridging carboxylate groups in an alternating way in **1**, whilst neighboring Co(II) ions are linked only by double  $\mu_{1,3}$ -bridging carboxylate groups in **2**. The carboxylate groups of

phthalate in **3** serve as a bridge between two Co(II) ions in  $\mu_2\text{-}\eta^1\text{:}\eta^1$  and  $\mu_1\text{-}\eta^1\text{:}\eta^0$  fashions. The large steric hindrance of the 3-position substituent group prevents the double bridged mode (Scheme 2C). For **4**, the nitro group does not coordinate to any Co(II) ion, and the ligand adopts  $\mu_2\text{-}\eta^1\text{:}\eta^1$  and  $\mu_1\text{-}\eta^1\text{:}\eta^0$  fashions to link three Co(II) ions into the final framework (Scheme 2D).

## 3.2. Magnetic studies

The magnetic susceptibilities of **1–4** were measured in the temperature range 2–300 K, as shown in Fig. S2. At room temperature, the  $\chi_{\text{M}}T$  values of 3.22 (**1**), 3.24 (**2**), 2.56 (**3**) and 3.26 (**4**)  $\text{cm}^3 \text{K mol}^{-1}$  are much higher than the expected 1.88  $\text{cm}^3 \text{K mol}^{-1}$  for the spin-only value of one free Co(II) ion ( $S = 3/2$ ), but the values are close to 3.38  $\text{cm}^3 \text{K mol}^{-1}$  ( $\chi_{\text{M}}T = N\beta^2/(3k) [L(L+1) + 4S(S+1)]$ ,  $L = 3$ ,  $S = 3/2$ ) where the contribution of the orbital angular momentum of the octahedral Co(II) ion is taken into account.

### 3.2.1. $[\text{Co}(\text{4apa})(\text{H}_2\text{O})]$ (**1**)

Upon cooling,  $\chi_{\text{M}}T$  decreases gradually until ca. 50 K and then it decreases rapidly to 0.16  $\text{cm}^3 \text{K mol}^{-1}$  at 2 K. A maximum value of 0.18  $\text{cm}^3 \text{mol}^{-1}$  at 5 K is observed for the magnetic susceptibility, suggesting possible antiferromagnetic interactions between the Co(II) ions. The data in the range 10–300 K obey the Curie–Weiss law [ $\chi_{\text{M}} = C/(T - \theta)$ ] with  $C = 3.5 \text{ cm}^3 \text{K mol}^{-1}$  and  $\theta = -23 \text{ K}$ . Though the orbital angular momentum of the hexacoordinated

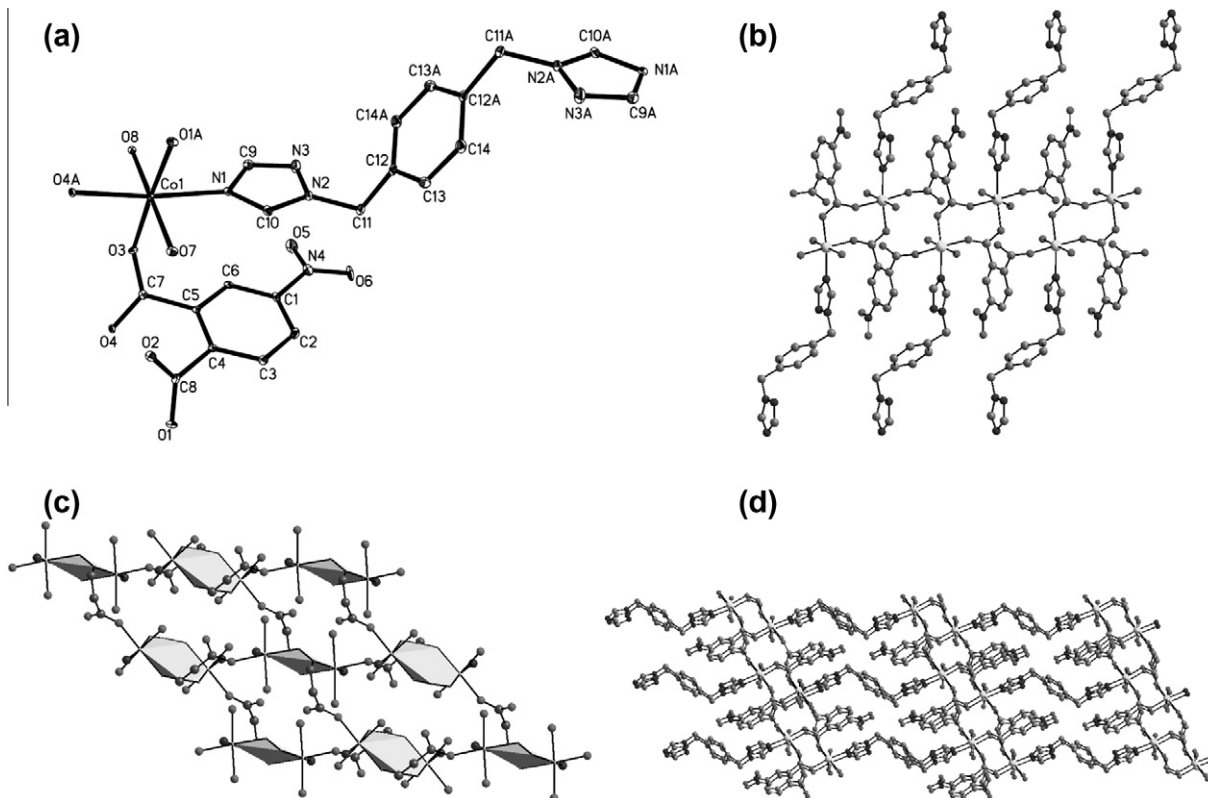
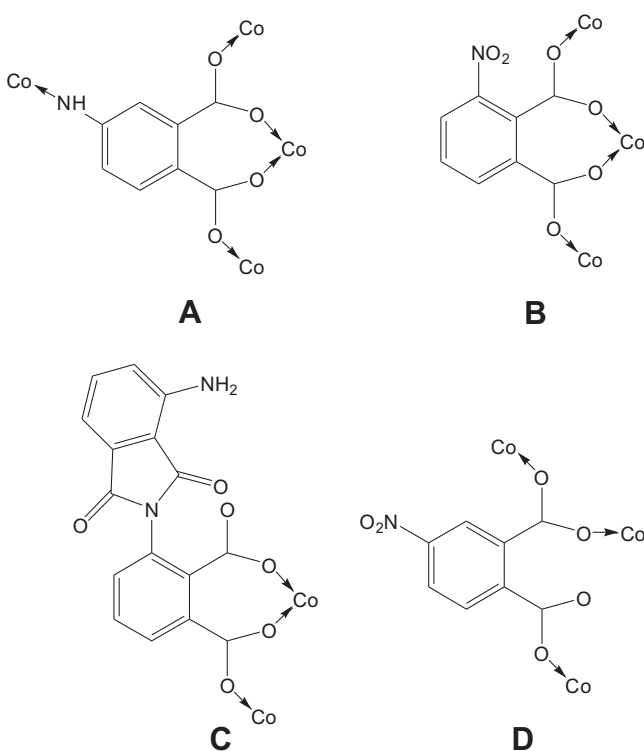


**Fig. 4.** (a) ORTEP plot of  $[\text{Co}(\text{btx})_{0.5}(\text{4npa})(\text{H}_2\text{O})_2]$  (**4**). Thermal ellipsoids are shown at 30% probability. (b) The 1D structure in **4**. (c) The 2D structure linked by carboxylate groups. (d) The 3D structure of **4**. All H atoms are omitted for clarity.



**Scheme 2.** Coordination modes of phthalic acid derivatives in **1** (A), **2** (B), **3** (C) and **4** (D).

high-spin Co(II) ions prevents quantitative analysis of the magnetic behavior by the spin Hamiltonian, an approximation is still possi-

ble. As shown in the crystallographic part (Fig. 1), **1** is comprised of a 2D structure in which each Co(II) ion is linked to the neighboring Co(II) ion by single or double *anti-syn* carboxylate bridges, with very small geometrical differences. The layers are further linked into a 3D framework by the  $4\text{apa}^{2-}$  ligands, which transmit much weaker magnetic coupling due to the long distance and  $\sigma$ -type C–N bond. Thus, from the magnetic point of view, the 3D structure can be reduced to a 2D magnetic structure. We analyzed the magnetic data with two methods. Firstly, if we assume that only one magnetic exchange parameter is necessary to study the coupling between the Co(II) ions, an approximate expression Eq. (1) [10] suitable for 1D/2D Co(II) complexes can be applied to estimate the magnetic interactions.

$$\chi_M T = A \exp\left(\frac{-E_1}{kT}\right) + B \exp\left(\frac{-E_2}{kT}\right) \quad (1)$$

In this expression,  $A + B$  equals the Curie constant, and  $E_1$ ,  $E_2$  represent “activation energies” corresponding to the spin-orbit coupling and the magnetic interaction, respectively. The best fit gave  $A + B = 3.5 \text{ cm}^3 \text{ K mol}^{-1}$ ,  $E_1/k = 63 \text{ K}$ ,  $E_2/k = 4.3 \text{ K}$ , ( $J = -3.0 \text{ cm}^{-1}$ ,  $\chi_M T \propto \exp(J/kT)$ ),  $R = 5.8 \times 10^{-5}$  ( $R = \sum[(\chi_M)_{\text{obs}} - (\chi_M)_{\text{calc}}]^2 / \sum[(\chi_M)_{\text{obs}}]^2$ ). Secondly, taking into account that double *anti-syn* carboxylate bridges may transmit stronger magnetic coupling than the single bridges, the magnetic structure can be considered as double-bridged dimers linked by single-bridged carboxylates. For this case, the Magsaki program [11] through a numerical matrix diagonalization based on the following Hamiltonian Eq. (2) suitable for a dimeric Co(II) system can be applied to fit the magnetic data (red dash line in Fig. S2(a)).

$$\hat{H} = -(3/2)\kappa\hat{L} \cdot \hat{S} + \Delta(\hat{L}_z^2 - L(L+1)/3) + \beta[-(3/2)\kappa\hat{L} + g_e\hat{S}] \cdot H - \hat{J}\hat{S}_1 \cdot \hat{S}_2 \quad (2)$$

**Table 3**  
Selected magneto-structural data for  $\mu_{1,3}$ -carboxylate bridged Co(II) complexes.

Compound <sup>a</sup>	Bridging mode	Nuclearity <sup>b</sup>	Fitting methods	C (cm <sup>3</sup> K mol <sup>-1</sup> )	$\Theta$ (K)	J (cm <sup>-1</sup> )	Ref.
[Co(btx)(IPA)]	<i>syn-syn</i>	dimer	$\chi_{Co} = \frac{Ng^2\beta^2}{k_B T} \frac{14+5X^6+X^{10}}{7+5X^6+3X^{10}+X^{12}} + TIP$ $X = \exp(-J/k_B T)$	3.30	-3.7	-0.12	[10a]
[Co <sub>3</sub> (btx) <sub>3</sub> (BTA) <sub>2</sub> (H <sub>2</sub> O) <sub>2</sub> ]	<i>syn-syn</i>	trimer	$\chi_{Co} = \frac{Ng^2}{3k_B T} \left\{ \frac{7(3-A)^2}{5} + \frac{12(A+2)^2}{25A} + \left[ \frac{2(11-2A)^2}{45} + \frac{176(A+2)^2}{675A} \right] \exp\left(\frac{5Ax}{2}\right) + \left[ \frac{(A+5)^2 x}{9} - \frac{20(A+2)^2}{27A} \right] \times \exp(-4Ax) \right\} /$ $\left\{ \frac{x}{3} \left[ 3 + 2 \exp\left(-\frac{5Ax}{2}\right) + \exp(-4Ax) \right] \right\} \chi_M = \chi_{Co} / [1 - \chi_{Co}(2zJ'/Ng^2\beta^2)]$	3.37	-8.4	-0.03	[10a]
[Co(ppdc)(H <sub>2</sub> O) <sub>2</sub> ] <sub>n</sub>	<i>anti-anti</i>	2D	$\mathbf{H} = -(25/9)J \sum_{i,j} \hat{S}_i^{\text{eff}} \cdot \hat{S}_j^{\text{eff}} - G(T,J) \beta H \sum_i \hat{S}_i^{\text{eff}}$	3.11	-13.3	-0.23	[13]
[Co <sub>2</sub> (4,4'-bpy)(Memal) <sub>2</sub> (H <sub>2</sub> O) <sub>2</sub> ] <sub>n</sub>	<i>anti-syn</i>	2D	$\chi_M = \frac{9N\beta^2}{25J} g_0^2 \left[ 3\Theta + \sum_{n=1}^6 \frac{C_n}{\Theta^n} \right]^{-1}$ $\Theta = 12k_B T / 25J$	-	-	-0.05	[14]
[Co(L <sup>1</sup> OO)(H <sub>2</sub> O)](ClO <sub>4</sub> ) <sub>2</sub> ·2H <sub>2</sub> O	<i>anti-syn</i>	1D	$\chi_M = \frac{N\beta^2 g^2}{k_B T} \frac{0.25 - 0.074975x + 0.075235x^2}{1.0 + 0.9931x + 0.172135x^2 + 0.757825x^3}$ $x = (25/9)J/k_B T$ ; G(T,J) function instead of the g factor	-	-	-2.65	[15]
[Co(bpe)(bba)] <sub>n</sub>	<i>anti-syn</i>	dimer	-	3.34	1.20	Ferro	[16]
[Co(4apa)(H <sub>2</sub> O)]	<i>anti-syn</i>	2D	$\chi_M T = A \exp\left(\frac{-E_1}{k_B T}\right) + B \exp\left(\frac{-E_2}{k_B T}\right)$	3.5	-23	-3.0	this work
[Co(bpy)(3npa)]	<i>anti-syn</i>	1D	$\chi_M T = A \exp\left(\frac{-E_1}{k_B T}\right) + B \exp\left(\frac{-E_2}{k_B T}\right)$	3.5	-19	-5.8	this work
[Co(bpy) <sub>1.5</sub> (3adpa)]	<i>anti-syn</i>	1D	$\chi_M T = A \exp\left(\frac{-E_1}{k_B T}\right) + B \exp\left(\frac{-E_2}{k_B T}\right)$	2.7	-17	-0.16	this work
[Co(btx) <sub>0.5</sub> (4npa)(H <sub>2</sub> O) <sub>2</sub> ]	<i>anti-syn</i>	dimer	$\hat{H} = -(3/2)k\lambda\hat{L} \cdot \hat{S} + \Delta(\hat{L}_z^2 - L(L+1)/3) + \beta[-(3/2)\kappa\hat{S} + g_e\hat{S}] \cdot H - J\hat{S}_1 \cdot \hat{S}_2$	3.5	-19	-0.12	this work
[Co <sub>3</sub> (ac) <sub>4</sub> (bpe) <sub>3</sub> (dca) <sub>2</sub> ] <sub>n</sub>	<i>syn-syn</i> & $\mu$ -oxo	trimer	$H = -2 \sum_{i=x,y,z} J_{1i}(S_{1i}S_{2i} + S_{2i}S_{3i})$ $S_{\text{eff}} = 1/2$	-	-	-1.6	[17]
[Co <sub>3</sub> (pybz) <sub>2</sub> (pico) <sub>2</sub> ] <sub>n</sub>	<i>syn-syn</i> & $\mu$ -oxo	2D	$\chi_M T = A \exp\left(\frac{-E_1}{k_B T}\right) + B \exp\left(\frac{-E_2}{k_B T}\right)$	2.96	-2.51	-1.4	[18]
[Co <sub>2</sub> (bta)(H <sub>2</sub> O) <sub>6</sub> ] <sub>n</sub> ·2nH <sub>2</sub> O	<i>syn-syn</i> & $\mu$ -oxo	dimer	$\hat{H} = -J\hat{S}_1\hat{S}_2 - \sum_{i=1}^2 \alpha_i \lambda_i \hat{L}_i \hat{S}_i + \sum_{i=1}^2 \Delta_i [\hat{L}_{zi}^2 - 2/3] + \beta H \sum_{i=1}^2 (-\alpha_i \hat{L}_i + g_e \hat{S}_i)$	-	-	+5.4	[7]
[Co(H <sub>2</sub> O)(phda)] <sub>n</sub> ·3nH <sub>2</sub> O	<i>syn-syn</i> & $\mu$ -oxo	dimer	$\hat{H} = \sum_{nn} -J\hat{S}_i\hat{S}_j - \sum_{nn} \alpha_i \lambda_i \hat{L}_i \hat{S}_i + \sum_{nn} \Delta_i [\hat{L}_{zi}^2 - 2/3] + \beta H \sum_{nn} (-\alpha_i \hat{L}_i + g_e \hat{S}_i)$	-	-	+2.11	[7]

<sup>a</sup> H<sub>2</sub>IPA = isophthalic acid, H<sub>3</sub>BTA = benzene-1,3,5-tricarboxylic acid, H<sub>2</sub>ppdc = p-phenylenediacrylic acid, Memal = methylmalonate dianion, L<sup>1</sup>OO = 3-[(2-(pyridin-2-yl)ethyl)(2-(pyridin-2-yl)methyl)amino]propionate, bpe = 1,2-bis(4-pyridyl)ethane, H<sub>2</sub>bba = isophthalic acid, dca = dicyanamide, ac = acetate, bpe = 1,2-bis-(4-pyridyl)ethane, pybz = 4-(pyridin-4-yl)benzoate, pico = 3-hydroxypicolinate, H<sub>4</sub>bta = 1,2,4,5-benzenetetracarboxylic acid, H<sub>2</sub>phda = 1,4-phenylenediacetic acid.

<sup>b</sup> The nuclearity of the compounds is based on the magnetic point of view.

In Eq. (2),  $\kappa$  is orbital reduction factor,  $\lambda$  is spin–orbit coupling parameter,  $\Delta$  is the axial splitting parameter,  $J$  is isotropic exchange interaction. The best fit gave  $J = -3.0 \text{ cm}^{-1}$ ,  $\kappa = 0.93$ ,  $\lambda = -130 \text{ cm}^{-1}$ ,  $\Delta = -351 \text{ cm}^{-1}$ ,  $g_z = 6.1$ ,  $g_x = 3.2$ ,  $\theta = -0.12 \text{ K}$ ,  $R(\chi) = 3.4 \times 10^{-3}$ ,  $R(\mu) = 1.0 \times 10^{-4}$  [ $R(\chi) = \sum(\chi_{\text{obsd}} - \chi'_{\text{caclid}})^2 / \sum(\chi_{\text{obsd}})^2$ ,  $R(\mu) = \sum(\mu_{\text{obsd}} - \mu'_{\text{caclid}})^2 / \sum(\mu_{\text{obsd}})^2$ ]. The negative  $J$  and  $\theta$  values suggest intradimer antiferromagnetic and interdimer antiferromagnetic interactions in **1**. Actually, the more the parameters, the more difficult it is to obtain both the reasonable parameters and the best fitting curve. The current fitting curve resembled to the experimental one as closely as possible, with all the parameters in a physically reasonable range.

### 3.2.2. [Co(bpy)(3npa)] (**2**)

Both the shapes of the  $\chi_M$  versus  $T$  curve and the  $\chi_M T$  versus  $T$  curve are similar to those of **1**. Upon cooling,  $\chi_M T$  decreases gradually until ca. 75 K and then drops to  $0.13 \text{ cm}^3 \text{ K mol}^{-1}$  at 2 K. A maximum is observed of  $0.11 \text{ cm}^3 \text{ mol}^{-1}$  at 10 K for the magnetic susceptibility. All these features suggest the possibility of an antiferromagnetic interaction between the Co(II) ions. Fitting the data (12–300 K) with Curie–Weiss law gave  $C = 3.5 \text{ cm}^3 \text{ K mol}^{-1}$  and  $\theta = -19 \text{ K}$ . Taking into account that the magnetic interaction between the Co(II) ions transmitted by  $\mu_{1,3}$  carboxylate groups in a 1D system should be larger than that of bpy in **2**, Eq. (1) was applied to fit the magnetic susceptibility data, and the fitting results are  $A + B = 3.5 \text{ cm}^3 \text{ K mol}^{-1}$ ,  $E_1/k = 51 \text{ K}$ ,  $E_2/k = 8.4 \text{ K}$ , ( $J = -5.8 \text{ cm}^{-1}$ ),  $R = 1.7 \times 10^{-3}$ . The results indicate the existence of antiferromagnetic interactions between adjacent Co(II) ions transmitted by the double  $\mu_{1,3}$  carboxylate groups.

### 3.2.3. [Co(bpy)<sub>1.5</sub>(3adpa)] (**3**)

The  $\chi_M T$  value decreases gradually to  $1.73 \text{ cm}^3 \text{ K mol}^{-1}$  at 12 K as the temperature decreases, and then increases to  $1.90 \text{ cm}^3 \text{ K mol}^{-1}$  at 2 K. The data (35–300 K) obey the Curie–Weiss law with  $C = 2.7 \text{ cm}^3 \text{ K mol}^{-1}$  and  $\theta = -17 \text{ K}$ . From a magnetic point of view, **3** could be considered as a 1D magnetic structure, though the crystal structure is 3D. The magnetic susceptibility data were fitted using Eq. (1). The best fit parameters were  $A + B = 2.8 \text{ cm}^3 \text{ K mol}^{-1}$ ,  $E_1/k = 59 \text{ K}$ ,  $E_2/k = 0.23 \text{ K}$ , ( $J = -0.16 \text{ cm}^{-1}$ ),  $R = 2.8 \times 10^{-4}$ . The negative and small  $J$  value suggests a weak antiferromagnetic interaction between adjacent Co(II) ions, transmitted by the  $\mu_{1,3}$  carboxylate groups.

### 3.2.4. [Co(btx)<sub>0.5</sub>(4npa)(H<sub>2</sub>O)<sub>2</sub>] (**4**)

The  $\chi_M T$  value decreases slightly to  $2.15 \text{ cm}^3 \text{ K mol}^{-1}$  on lowering the temperature to 7 K. Below this temperature,  $\chi_M T$  increases to a value of  $2.22 \text{ cm}^3 \text{ K mol}^{-1}$  at 2 K. The shape of the  $\chi_M T$  versus  $T$  curve is similar to that of **3**. Fitting the data (35–300 K) to the Curie–Weiss law gave  $C = 3.5 \text{ cm}^3 \text{ K mol}^{-1}$  and  $\theta = -19 \text{ K}$ . Taking into account the dimeric structure in **4**, the Magsaki program was applied to fit the magnetic data for a quantitative estimation of the magnetic interaction. The best fit gives  $J = -0.12 \text{ cm}^{-1}$ ,  $\kappa = 0.93$ ,  $\lambda = -136 \text{ cm}^{-1}$ ,  $\Delta = -632 \text{ cm}^{-1}$ ,  $g_z = 7.0$ ,  $g_x = 2.5$ ,  $\theta = 0.18 \text{ K}$ ,  $\text{TIP} = 6.7 \times 10^{-4} \text{ cm}^3 \text{ mol}^{-1}$ ,  $R(\chi) = 3.4 \times 10^{-4}$ ,  $R(\mu) = 1.8 \times 10^{-5}$  for **4**. The negative and small  $J$  value suggests a weak antiferromagnetic interaction in the dimer, transmitted by the double  $\mu_{1,3}$  carboxylate groups. For **3** and **4**, the  $\chi_M T$  curve shows a small upturn at low temperatures. This increase may be a consequence of weak ferromagnetic coupling resulting from spin-canting.

$\mu_{1,3}$ -Carboxylate bridged Cu(II) complexes can adopt different conformations (*syn–syn*, *anti–syn* and *anti–anti*) and the ferro- or antiferro-magnetic interactions between the Cu(II) centers have been thoroughly investigated [12]. In contrast, the study of magneto-structural correlations of  $\mu_{1,3}$ -carboxylate bridged Co(II) complexes is rather rare due to the difficulties in both their synthesis and analysis of the magnetic susceptibility. Herein, the carboxylate

groups assume a triatomic *anti–syn* bridging conformation in **1–4**. Based on the magnetic data, the large and negative Weiss constants indicate not only spin–orbit coupling of the Co(II) ions, but also significant antiferromagnetic interactions between the Co(II) ions bridged by double  $\mu_{1,3}$ -carboxylate groups in **1** and **2**, which is further confirmed by quantitative analysis of the data. Analysis of the magnetic data for **3** and **4** suggests weak antiferromagnetic interactions between the Co(II) ions bridged by single  $\mu_{1,3}$ -carboxylate groups. The relevant magneto-structural data, including the bridging mode together with the exchange parameters, for selected  $\mu_{1,3}$ -carboxylate bridged Co(II) complexes are listed in Table 3. A few examples show weak antiferromagnetic interactions across the *syn–syn* conformation, and most of the examples possess antiferromagnetic interactions through the *anti–anti* and *anti–syn* conformations. Our work also shows that the double-bridging mode always leads to larger magnetic interactions compared to the single-bridging mode, which is similar to the case of Cu(II) species.

## 4. Conclusions

In summary, by using phthalic acid derivatives as ligands, four Co(II) coordination polymers have been synthesized and structurally characterized. In the four coordination polymers, the adjacent Co(II) ions are bridged by  $\mu_{1,3}$  carboxylate groups in the *anti–syn* mode to form 2D (**1**), 1D (**2** and **3**) and dimer (**4**) magnetic structures, which are linked into 3D crystal structures. The different 3D structures, as well as the magnetic structures, come from the different substituent group and/or the co-ligands. It is noted that an interesting *in situ* acylation reaction was observed in the formation of coordination polymer **3**. Magnetic studies reveal antiferromagnetic interactions between the Co(II) ions in **1–4**. This work shows a strategy to tune the subtle bridging mode to influence the magnetic configuration, which will lead to the development of new molecular magnetic materials.

## Acknowledgments

This work was supported by the National Natural Science Foundation of China (21151001, 21171100 and 90922032) and the Fundamental Research Funds for the Central Universities.

## Appendix A. Supplementary material

CCDC 884148–884151 contain the supplementary crystallographic data for **1–4**. These data can be obtained free of charge via <http://www.ccdc.cam.ac.uk/conts/retrieving.html>, or from the Cambridge Crystallographic Data Centre, 12 Union Road, Cambridge CB2 1EZ, UK; fax: +44 1223 336 033; or e-mail: deposit@ccdc.cam.ac.uk. Supplementary data associated with this article can be found in the online version, at <http://dx.doi.org/10.1016/j.poly.2012.12.032>.

## References

- [1] (a) O. Kahn, *Molecular Magnetism*, VCH, New York, 1993; (b) J.S. Miller, M. Drillon, *Magnetism: Molecules to Materials*, Wiley-VCH, Weinheim, 2001; (c) M. Kurmoo, *Chem. Soc. Rev.* 38 (2009) 1353; (d) D.F. Weng, Z.M. Wang, S. Gao, *Chem. Soc. Rev.* 40 (2011) 3157; (e) P. Dechambenoit, J.R. Long, *Chem. Soc. Rev.* 40 (2011) 3249; (f) A. Caneschi, D. Gatteschi, N. Lalioti, C. Sangregorio, R. Sessoli, G. Venturi, A. Vindigni, A. Rettori, M.G. Pini, M.A. Novak, *Angew. Chem., Int. Ed.* 40 (2001) 1760; (g) R. Clérac, H. Miyasaka, M. Yamashita, C. Coulon, *J. Am. Chem. Soc.* 124 (2002) 12837.
- [2] (a) B. Zhao, X.Y. Chen, P. Cheng, D.Z. Liao, S.P. Yan, Z.H. Jiang, *J. Am. Chem. Soc.* 126 (2004) 15394; (b) R. Fu, S. Xiang, S. Hu, L. Wang, Y. Li, X. Huang, X. Wu, *Chem. Commun.* 42 (2005) 5292;

- (c) M.D. Allendorf, C.A. Bauer, R.K. Bhakta, R.J.T. Houk, *Chem. Soc. Rev.* 38 (2009) 1330.
- [3] (a) J. Lee, O.K. Farha, J. Roberts, K.A. Scheidt, S.T. Nguyen, J.T. Hupp, *Chem. Soc. Rev.* 38 (2009) 1450;  
(b) L.Q. Ma, C. Abney, W.B. Lin, *Chem. Soc. Rev.* 38 (2009) 1248;  
(c) Z. Zhang, L. Zhang, L. Wojtas, P. Nugent, M. Eddaoudi, M.J.J. Zaworotko, *J. Am. Chem. Soc.* 134 (2012) 928.
- [4] (a) J.R. Li, R.J. Kuppler, H.C. Zhou, *Chem. Soc. Rev.* 38 (2009) 1477;  
(b) K. Sumida, C.M. Brown, Z.R. Herm, S. Chavan, S. Bordiga, J.R. Long, *Chem. Commun.* 47 (2011) 1157;  
(c) S.A.K. Robinson, M.-V.L. Mempin, A.J. Cairns, K.T. Holman, *J. Am. Chem. Soc.* 133 (2011) 1634;  
(d) Q. Lin, T. Wu, S.T. Zheng, X. Bu, P. Feng, *J. Am. Chem. Soc.* 134 (2012) 784.
- [5] (a) X.Y. Wang, Z.M. Wang, S. Gao, *Chem. Commun.* (2008) 281;  
(b) C. Adhikary, S. Koner, *Coord. Chem. Rev.* 254 (2010) 2933;  
(c) S. Wang, X.H. Ding, Y.H. Li, W. Huang, *Coord. Chem. Rev.* 256 (2012) 439;  
(d) T.C. Stamatatos, C.G. Efthymiou, C.C. Stoumpos, S.P. Perlepes, *Eur. J. Inorg. Chem.* (2009) 3361;  
(e) J. Ferrando-Soria, R. Ruiz-Garcia, J. Cano, S.-E. Stiriba, J. Vallejo, I. Castro, M. Julve, F. Lloret, P. Amoros, J. Pasan, C. Ruiz-Perez, Y. Journaux, E. Pardo, *Chem. Eur. J.* 18 (2012) 1608.
- [6] (a) Y. Oka, K. Inoue, *Chem. Lett.* 33 (2004) 402;  
(b) P. Mahata, M. Prabu, S. Natarajan, *Inorg. Chem.* 47 (2008) 8451;  
(c) X.M. Zhang, Z.M. Hao, W.X. Zhang, X.M. Chen, *Angew. Chem., Int. Ed.* 46 (2007) 3456;  
(d) M.X. Yao, M.H. Zeng, H.H. Zou, Y.L. Zhou, H. Liang, *Dalton Trans.* (2008) 2428;  
(e) P. Albores, E. Rentschler, *Dalton Trans.* (2009) 2609.
- [7] O. Fabelo, L. Canadillas-Delgado, J. Pasan, F.S. Delgado, F. Lloret, J. Cano, M. Julve, C. Ruiz-Perez, *Inorg. Chem.* 48 (2009) 11342.
- [8] (a) S.G. Baca, I.G. Filippova, O.A. Gherco, M. Gdaniec, Y.A. Simonov, N.V. Gerbeleu, P. Franz, R. Basler, S. Decurtins, *Inorg. Chim. Acta* 357 (2004) 3419;  
(b) D.R. Xiao, E.B. Wang, H.Y. An, Y.G. Li, Z.M. Su, C.Y. Sun, *Chem. Eur. J.* 12 (2006) 6528;  
(c) S.Y. Zhang, W. Shi, Y. Lan, N. Xu, X.Q. Zhao, A.K. Powell, B. Zhao, P. Cheng, D.Z. Liao, S.P. Yan, *Chem. Commun.* 47 (2011) 2859.
- [9] (a) G.M. Sheldrick, *SHELXS 97*, Program for the Solution of Crystal Structures, University of Göttingen, Germany, 1997;  
(b) G.M. Sheldrick, *SHELXL 97*, Program for the Refinement of Crystal Structures, University of Göttingen, Germany, 1997.
- [10] (a) J.M. Rueff, N. Masciocchi, P. Rabu, A. Sironi, A. Skoulios, *Chem. Eur. J.* 8 (2002) 1813;  
(b) L.A. Barrios, J. Ribas, G. Arom, J. Ribas-Ario, P. Gamez, O. Roubeau, S.J. Teat, *Inorg. Chem.* 46 (2007) 7154;  
(c) H.S. Yoo, J.I. Kim, N. Yang, E.K. Koh, J.G. Park, C.S. Hong, *Inorg. Chem.* 46 (2007) 9054;  
(d) S.Y. Zhang, Z.J. Zhang, W. Shi, B. Zhao, P. Cheng, D.Z. Liao, S.P. Yan, *Dalton Trans.* 40 (2011) 7993.
- [11] (a) H. Sakiyama, *J. Chem. Software* 7 (2001) 171;  
(b) H. Sakiyama, *J. Comput. Chem. Jpn.* 6 (2007) 123.
- [12] (a) M. Kato, Y. Muto, *Coord. Chem. Rev.* 92 (1988) 45;  
(b) E. Colacio, J.M. Domínguez-Vera, M. Ghazi, R. Kivekas, M. Klinga, J.M. Moreno, *Eur. J. Inorg. Chem.* (1999) 441;  
(c) A. Rodríguez-Forteza, P. Alemany, S. Alvarez, E. Ruiz, *Chem. Eur. J.* 7 (2001) 627.
- [13] Q. Sun, A.L. Cheng, Y.Q. Wang, Y. Ma, E.Q. Gao, *Inorg. Chem.* 50 (2011) 8144.
- [14] M. Deniz, J. Pasan, O. Fabelo, L. Canadillas-Delgado, F. Lloret, M. Julvec, C. Ruiz-Perez, *New J. Chem.* 34 (2010) 2515.
- [15] H. Arora, F. Lloret, R. Mukherjee, *Inorg. Chem.* 48 (2009) 1158.
- [16] T. Han, P. Ren, N. Xu, P. Cheng, D.Z. Liao, S.P. Yan, *Inorg. Chim. Acta* 387 (2012) 212.
- [17] D. Ghoshal, G. Mostafa, T.K. Maji, E. Zangrando, T.H. Lu, J. Ribas, N.R. Chaudhuri, *New J. Chem.* 28 (2004) 1204.
- [18] M.H. Zeng, Y.L. Zhou, M.C. Wu, H.L. Sun, M. Du, *Inorg. Chem.* 49 (2010) 6436.